Localizer with high occlusion immunity using diffraction optics

Thomas D. Ditto[*] and Jacques Farges [a]

[a]Silicon Vision, 2996 Venables Street, Vancouver, B.C., Canada, V5K 2R9

ABSTRACT

The chromatic method of diffraction range finding can be exploited to construct a 3D localizer that tracks the position of a pointer, a 3-D scanner or a robotic end-effecter. A spectrogram is made using a diffraction grating as the primary objective of an optical system that tracks a broad band emitter such as a tungsten filament or white L.E.D. Image processing on the resulting spectra transforms the spectrogram at the input to distance and displacement at the output. The behavior conforms to geometric optics following the Diffraction Equation. This novel technique has unique features. For example, the number of samples increases with target distance, reversing the loss of resolution as a function of distance that is endemic to triangulation. The plurality of samples also can overcome occlusion liability common to time-of-flight range finders, since multiple paths exist between emitter and sensor. The grating can be made from inexpensive embossed plastic, and a wave length sensor can be constructed from garden variety color cameras. The method is robust at a grazing exodus angles that allow for a compact configuration of the receiver. In this paper we disclose the theory of operation including a mathematical model, and we demonstrate the method empirically.

Keywords: 3-D, diffraction, holography, spectroscopy, localizer

1. PRIOR ART

Hand held profilometers and robotic end effectors are controlled in closed loop operations by spatial trackers called localizers. Robotic arms are motorized with encoded motors, and a common derivative embodiment, the Co-ordinate Measurement Machine (CMM), is localization by means of articulated arms with encoded wheels at the joints. Accuracy and repeatability of can be high, but rigid members restrain mobility. Increased flexibility is obtained only at the expense of adding many flexible elbows, an expensive step not taken in garden variety CMM's.

Magnetic wave detectors can serve as localizers in non ferrous environments. Indeed, when magnetic metals are absent, the magnetic wave detector has no occlusion liability, because magnetic lines-of-force pass through line-of-sight obstructions. Compared to CMM probes, the magnetic wave method has noise, low accuracy and poor repeatability. Magnetic wave accuracy is inversely proportional to target distance.

Ultrasonic detectors are time-of-flight detectors and have uniform accuracy at any working distance. Despite this desirable feature, commercial units have always suffered overall from low accuracy and repeatability, limited range, and environmental interference. Unlike magnetic wave devices, sonar localizers require an unoccluded line-of-sight to the target, but they do not suffer from an occlusion liability common to all triangulation devices where transmitter and receiver have separate paths.

Triangulation localizers are line-of-sight types that have occlusion liability in the paths of at least two sight lines. Multiple camera arrays can provide redundancy to improve occlusion immunity, but complexity and cost grow while speed of acquisition declines. Although triangulation accuracy can be very high within a very restricted work area, broad coverage sacrifices accuracy. Like magnetic wave localization, triangulation accuracy is inversely proportional to distance. If a stand-off to target increases, accuracy can only be maintained by increasing stereoscopic spacing, but in the process, field-of-view or accuracy are inevitably lowered.

1.1. Diffraction Range Finding

A useful phenomenon not heretofore exploited called diffraction range finding postulates that the appreciable curvature of a wave front incident upon a diffraction grating controls the displacement of higher-order diffraction spectra.

[*] 3d@taconic.net

Diffraction orders collapse into the zero-order at the grating plane itself, and they reach their greatest separation when the source of incident radiation is at infinity. In almost all spectrometers, an incoming wave front is collimated into a plane wave in order to assure that the displacement of resulting wavelengths is expanded to the asymptotic limit afforded by a spectrometer's diffraction grating.

However, without collimating optics at the input, a spectrometer is effectively also range finder, because the displacement of the higher-order spectra happens to be inversely proportional to the range of the source of illumination. The exploitation of the phenomenon is noted as the principal claim of the 1987 US patent, Range Finding by Diffraction

> A method for determining range by correlating the relationship between the distances of a diffraction grating from an illuminated target surface with the respective displacements of the high order diffraction images from the position of the respective zero order image as observed through said grating.[1]

A prototype hand held 3D profilometer dubbed "Moly" was built to demonstrate how this principle can be exploited by a measurement of the first-order displacement of a single monochromatic sheet of laser light when imaged through a chirped holographic grating.[2] Tabletop demonstrations of Moly were given at the 3DIM conferences in 1997, 1999,and 2001. A paper was published in 3DIM200l *Proceedings*. [3] Like other hand held profilometers, Moly required the use of a localizer. A magnetic wave type was used. In practice the magnetic device offered no better than millimeter repeatable resolution. This compared to a measure of ~100 microns made in each profile by the diffraction method prototype. The question was raised as to whether the diffraction method itself could be exploited for localization

2. CHROMATIC DIFFRACTION RANGE FINDING METHOD

The measured parameter in the diffraction profilometer prototype "Moly" is the displacement of the higher-order diffraction image of a monochromatic sheet of laser light. However, if a broad spectrum illuminates the target, range can be acquired by measuring the resulting spectrum for its color information. In short, the color of diffracted light corresponds to the distance of a source of illumination.

When color is the measured parameter of a diffraction range finder, a single color reading can determine target distance. Color readings can be taken with bi-stimulus or tri-stimulus cells. Red-Green-Blue (RGB) triads are typical, because they mimic the human eye. Compared to the type of spatial displacement measurement used in "Moly", the chromatic method can be implemented with far fewer sensor cells in the receiver. Alternatively, if many sensor cells are used, a chromatic diffraction range finder enjoys benefits in accuracy and occlusion immunity over competing methods.

2.1 Principle of Chromatic Diffraction Ranging

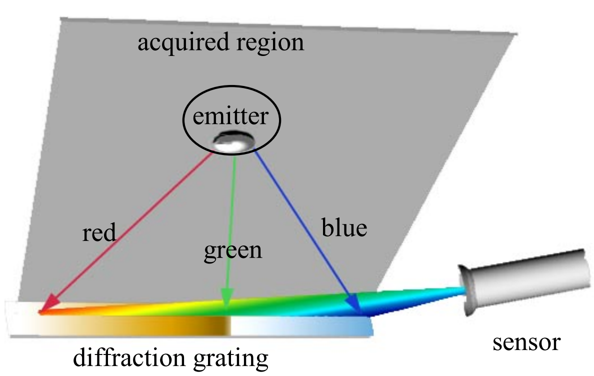

Figure 1 White light from a point source emitter is dispersed across the considerable length of a grating. This example is illustrated with a reflection type grating.

A diffraction grating disperses light from a point source into the lens of a sensor at an angle conforming to the diffraction equation. For the example shown in Figure 1, red light would be to the left, green to the middle and blue to the right.

The phenomenon exploited by the chromatic method is that as a source of illumination moves toward the grating, the spacing between spectra will collapse, until all spectra appear at the same site when at point-of-contact.

When an emitter is translated in the axis of the grating, the spectra shift proportionately. At a fixed emitter distance, spacing of higher-order spectra remains constant.

2.2 Mathematical Model

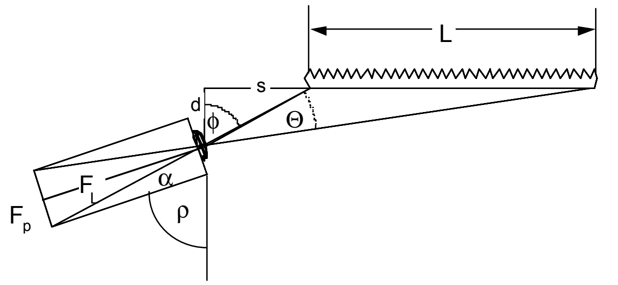

Figure 2 Receiver and grating model

For any configuration of grating length L, the distance below the grating plane to a camera lens is distance d. The lens has a focal length F_L and the camera has a sensor array on a focal plane of size F_P. To capture the grating from end to end, the camera must be positioned at a stand-off s and rotated toward the grating at angle ϕ. We can calculate s where d is given or d where s is given, and ϕ can be determined once s and d are known. Refer to Figure 2.

Inside the camera there are triangles such that

(1) $$\frac{\frac{F_P}{2}}{F_L} = \tan\left(\frac{\Theta}{2}\right)$$

The field-of-view Θ afforded by a lens focused at infinity is therefore

(2) $$\Theta = 2\arctan\left(\frac{1}{2}\frac{F_P}{F_L}\right)$$

The field-of-view covers the grating exclusively so

(3 & 4) $$\tan(\phi) = \frac{s}{d} \quad \text{and} \quad \tan(\phi + \Theta) = \frac{s+L}{d}$$

Taking advantage of the equivalency on d

(5) $$\frac{s+L}{\tan(\phi+\Theta)} = \frac{s}{\tan(\phi)}$$

The trigonometric identity for $\tan(\phi+\Theta)$ gives us

(6) $$\phi = \arctan\left[\frac{L + \sqrt{L^2 + 4s^2\tan(\Theta)^2 - 4Ls\tan(\Theta)^2}}{2s\tan(\Theta) - 2L\tan(\Theta)}\right]$$

Now suppose d is a given design parameter rather than stand-off s. A similar derivation is possible using the equivalency

(7) $$s = d\tan(\phi)$$

(8) $$s = d\left(\tan(\phi+\Theta) - \frac{L}{d}\right)$$

As with (6) one can solve for ϕ . This solution, like (6), is the positive root.

(9) $$\phi = \arctan\left[\frac{L\tan(\Theta) - \sqrt{\tan(\Theta)\left(L^2\tan(\Theta) - 4d^2\tan(\Theta) + 4dL\right)}}{2d\tan(\Theta)}\right]$$

As illustrated in Figure 3, consider a measurement of the displacement of a target along the (y,z) axes as detected at the camera by the movement of the color images on the focal plane measured at axis x with its origin corresponding to the intersection of the (y,z) axes. The deflection x of the image across F_P is inscribed by angle θ. With ϕ also known, we can then find the angle r at which the grating diffracts a wave front originating from a target at (y,z).

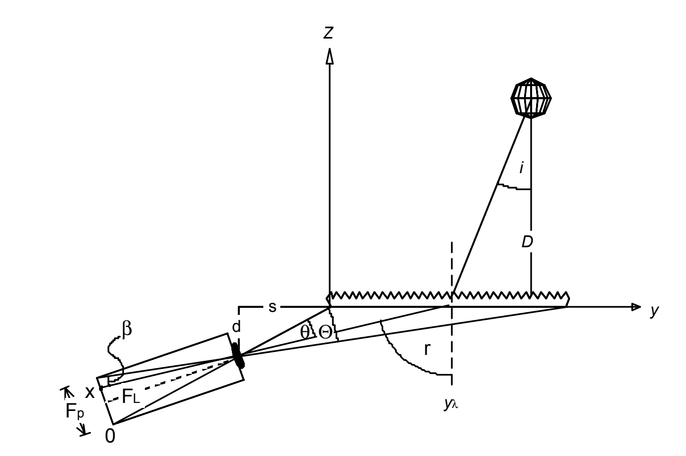

Figure 3 Receiver, grating and target model

10) $$r = \theta + \phi$$

To find θ, an inscribed angle β will first be calculated:

(11) $$\beta = \arctan\left(\frac{\frac{F_P}{2}}{F_L}\right) - \arctan\left(\frac{x - \frac{F_p}{2}}{F_L}\right)$$

(12) $$\theta = \Theta - \beta$$

Substituting (2) into (11)

(13) $$\theta = \Theta - \frac{\Theta}{2} + \arctan\left(\frac{x - \frac{F_p}{2}}{F_L}\right)$$

The legs opposed to angle r can be used to obtain:

(14) $$\tan(r) = \frac{s + y_\lambda}{d}$$

(15) $$y_\lambda = d\left(\tan(r) - \frac{s}{d}\right)$$

Substituting Equation (13) into Equation (15)

(16) $$y_\lambda = d\left[\tan\left(\left(\Theta - \frac{\Theta}{2} + \arctan\left(\frac{x_\lambda - \frac{F_P}{2}}{F_L}\right)\right) + \phi\right) - \frac{s}{d}\right]$$

By (16) it is possible to use the measured variable x, displacement on a focal array to be used to locate a corresponding point y_λ on the grating plane.

The Diffraction Equation is then invoked.

(17) $$\sin(r) + \sin(i) = n\frac{\lambda}{p}$$

where n is the diffraction-order, an integer
p is the grating pitch

Solving for the angle of incidence, i,

(18) $$i = \arcsin\left(n\frac{\lambda}{p} - \sin(r)\right)$$

The geometry in Figure 3 illustrates that, for any arbitrary diffraction spectral color λ appearing along the grating plane at y_λ, there is an incident diffraction angle i at distance D (where D is the target range) such that

(19) $$\tan(i) = \frac{y - y_\lambda}{D}$$

From (19) the solution for y for any case of y_λ is

(20) $$y = D \tan(i) - y_\lambda$$

As illustrated in Figure 4, in the case of two values for y_λ made with readings at two wave lengths λ_1 and λ_2 it follows from Equation (20) that

(21) $$D \tan(i_1) - y_{\lambda 1} = D \tan(i_2) - y_{\lambda 2}$$

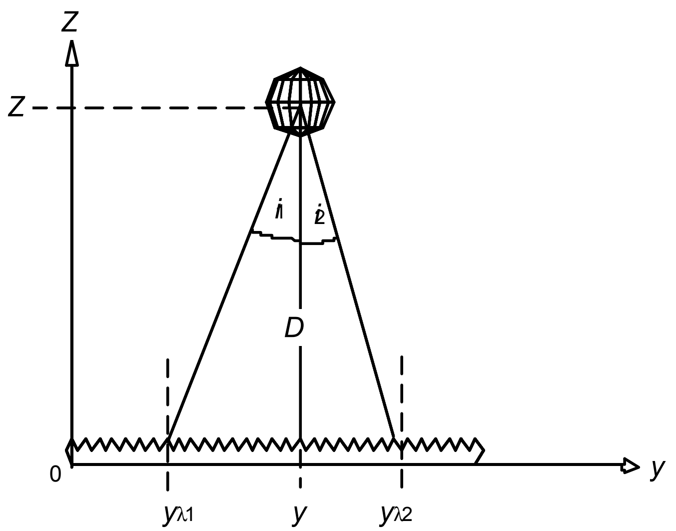

Figure 4 Target side of grating with two spectral lines indicated as λ_1 and λ_2

Target range D and displacement at co-ordinate y can be found, first by finding the range D at co-ordinate y where two measurements are made for λ at the focal plane. First

(22) $$D = \frac{y_{\lambda 1} - y_{\lambda 2}}{\tan(i_1) - \tan(i_2)}$$

Then with D known, the displacement y can be calculated with either

(23) $$y = D \tan(i_1) - y_{\lambda 1}$$

or

(24) $$y = D \tan(i_2) - y_{\lambda 2}$$

These equations can be applied to all rgb readings at all active photosites on the focal plane, allowing for many redundant data points appropriate for statistical methods that reduce error.

2.3 Sample Calculation

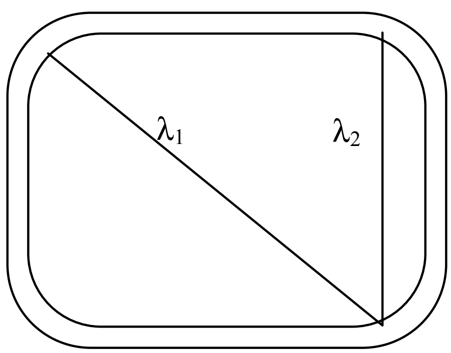

Figure 5 Area focal array image of two focal lengths

Consider a case where a selected wavelength λ_1 shifts uniformly across the focal plane of a color camera while another wavelength λ_1 stays at a fixed position on one side of the focal plane.

The variation in the position of λ_1 as illustrated in Figure 5 will predict the change in the range of the target:

- grating pitch: p = 600 nm grating length L = 150 mm
- wavelengths: λ_1 = 420 nm λ_2 = 650 nm
- Lens focal length F_L = 50 mm Focal Plane F_P = 6.4 mm
- Lens elevation over grating d = 40 mm
- Iterators: M = 50 j = 1…M

We use Mathcad 6 for the calculation in the box Figure 6.

$$\Theta := 2\cdot \mathrm{atan}\left(\frac{1}{2}\cdot\frac{F_P}{F_L}\right)$$

$$\phi := -\mathrm{atan}\left(\frac{L\cdot\tan(\Theta) - \sqrt{\tan(\Theta)}\cdot\sqrt{L^2\cdot\tan(\Theta) - 4\cdot d^2\cdot\tan(\Theta) + 4\cdot d\cdot L}}{2\cdot d\cdot\tan(\Theta)}\right)$$

$$s := d\cdot\tan(\phi)$$

$$\rho := \phi + \mathrm{atan}\left(\frac{F_P}{2\cdot F_L}\right)$$

$$\frac{\Theta}{deg} = 7.324 \quad \frac{\phi}{deg} = 75.086 \quad \frac{\rho}{deg} = 78.748 \quad \frac{s}{mm} = 150.184$$

$$x_{\lambda 1_j} := \frac{F_P}{M}\cdot j \qquad x_{\lambda 2} := F_P$$

$$\beta_{\lambda 1_j} := \mathrm{atan}\left(\frac{F_P}{2\cdot F_L}\right) - \mathrm{atan}\left(\frac{2\cdot x_{\lambda 1_j} - F_P}{2\cdot F_L}\right)$$

$$\beta_{\lambda 2} := \mathrm{atan}\left(\frac{F_P}{2\cdot F_L}\right) - \mathrm{atan}\left(\frac{2\cdot x_{\lambda 2} - F_P}{2\cdot F_L}\right)$$

$$\theta_{\lambda 1_j} := \Theta - \beta_{\lambda 1_j} \qquad \theta_{\lambda 2} := \Theta - \beta_{\lambda 2}$$

$$r_{\lambda 1_j} := \phi + \theta_{\lambda 1_j} \qquad r_{\lambda 2} := \phi + \theta_{\lambda 2}$$

$$y_{\lambda 2} := \left(\tan\left(r_{\lambda 2}\right) - \frac{s}{d}\right)\cdot d \qquad y_{\lambda 1_j} := \left(\tan\left(r_{\lambda 1_j}\right) - \frac{s}{d}\right)\cdot d$$

$$i_{\lambda 1_j} := \mathrm{asin}\left(\frac{\lambda_1}{p} - \sin\left(r_{\lambda 1_j}\right)\right) \qquad i_{\lambda 2} := \mathrm{asin}\left(\frac{\lambda_2}{p} - \sin\left(r_{\lambda 2}\right)\right)$$

$$D_j := \frac{y_{\lambda 2} - y_{\lambda 1_j}}{\left(\tan\left(i_{\lambda 2}\right) - \tan\left(i_{\lambda 1_j}\right)\right)}$$

$$y_{a_j} := y_{\lambda 1_j} - D_j\cdot\tan\left(i_{\lambda 1_j}\right) \qquad y_{b_j} := y_{\lambda 2} - D_j\cdot\tan\left(i_{\lambda 2}\right)$$

Figure 6 Mathcad 6 worksheet for sample calculation

We use the same sequence of steps in a Mathcad calculation to make a prediction for a set of ranges where λ_1 and λ_2 converge as per Figure 8. The predicted result is illustrated in Figure 9.

The result of the calculation is illustrated in the graph of Figure 7. The predicted collapse of the higher-order images into each other occurs as the two measured wavelengths merge on the right hand side of the image.

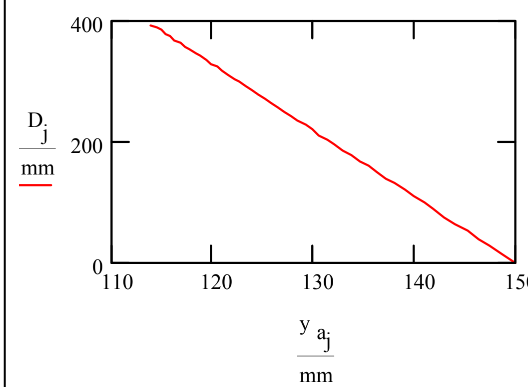

Figure 7 Displacement y and range D as per Figures 5 & 6

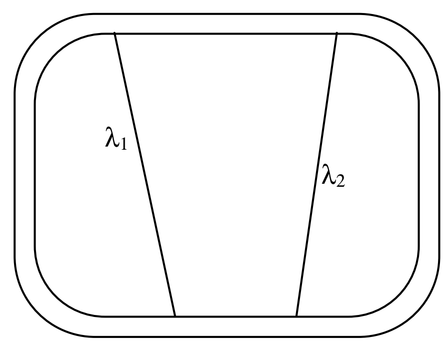

Figure 8 Area focal image where both wavelengths change in displacement.

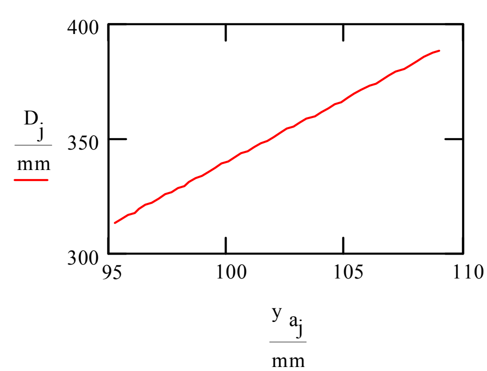

Figure 9 Displacements predicted as per Figure 8

3 Embodiments

The novel method of chromatic diffraction range finding will be exploited in configurations that address the specific needs of localization. These include volume of coverage, resolution, calibration, and enclosure.

3.1 Grazing exodus

A grazing exodus angle of the measured diffraction higher-order gives leverage to the far-field magnification of targets. Additionally, the placement of the sensor at a grazing angle vastly compacts an instrument over configurations where the sensor is placed away from the grating plane. Localization devices may be required to acquire volumes that have meter scale dimensions. Grazing exodus allows a diffraction grating to assume a long yet narrow aspect ratio. When a sensor is placed close to the grating plane, it can be configured to encompass both the frontal and the distal *extrema* of a grating.

In order for a working volume to be acquired, the target must be seen even as it translates through a field, even if only a line is acquired. To do this, a long thin grating can be wrapped around a cylinder. The embodiment is shown in Figure 10.

When linear detectors are used as the sensor, a second axis must be installed as per Figure 11 in order to acquire all three dimensions.

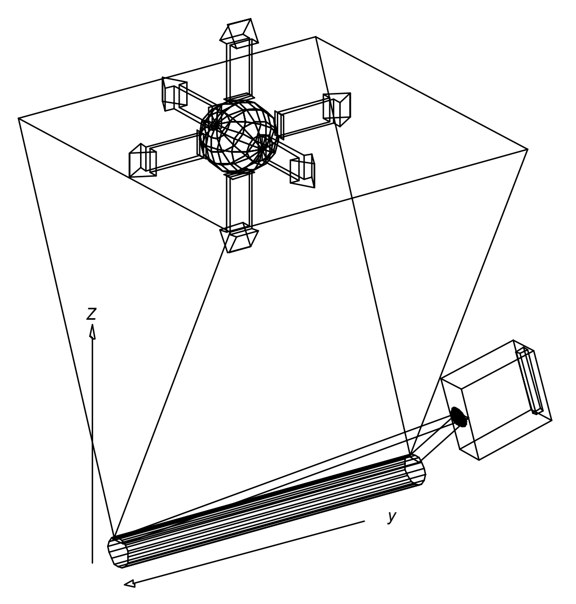

Figure 10 Grazing exodus receiver and cylindrical grating substrate form a working volume of acquisition

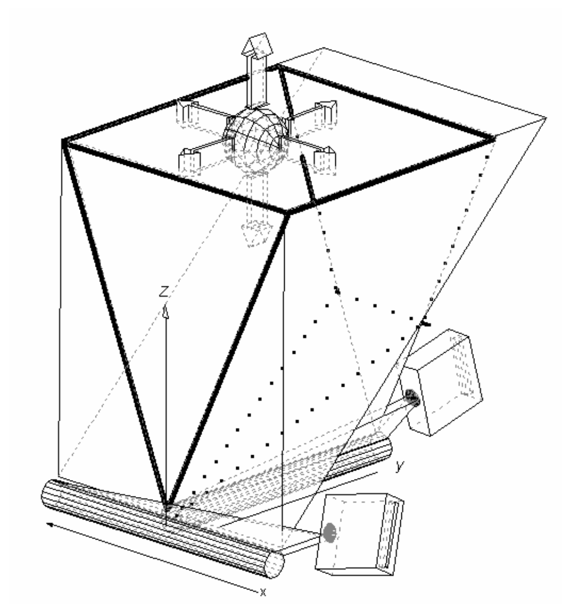

Figure 11 A pair of linear sensors used with orthogonal gratings on cylinder substrates to acquire a working volume

3.2 Color

Correlation of color to distance previously appeared in triangulation systems. The 1977 Pantomation[4] system created by one the present authors was notable for the color tags used to track body movement. A video chroma keyer under computer control was used to detect the color tags. Tag range distance could be determined through the use of two cameras. The rainbow system developed by NEC in the late 1980's used a diffraction grating in the projector and a color sensor as the receiver. [5] A derivative rainbow system is now commercially marketed by Genex.[6] All prior systems differ from the chromatic diffraction method in that a unique color is applied to the target surface rather than extracted from a broad band source imaged by the receiver. The NEC and Genex systems form an interesting contrast with the present technique since the former uses a projected spectrum whereas the latter extracts the spectrum with a diffraction grating in the camera.

Color-based ranging systems must accommodate ambiguous colors called metamers, a pair of colors which differ spectrally but which yield the same or similar tri-stimulus values under at least one set of viewing conditions. The gold standard for color discrimination is spectroscopy by dispersion using either a diffraction grating or a prism, and the data provided by the grating in a chromatic diffraction range finder will be spectrally pure, once metamers are removed. Where color discrimination is made by means of a series of band pass filters such as red, green and blue, the color temperature of the source must be accommodated, and the ambient environment must be subtracted out. These are well understood practices in science of colorimetry.[7]

Once metamers are removed, the range discrimination of a chromatic diffraction range finder is determined, in part, by the bit depth of the color sensor. The conversion of color to wavelength is effective over the region where the Gaussian distribution of color intensities of bandpass filters overlap.

3.3 Demonstration

Experimental study of the chromatic method of diffraction range finding has proceeded using inexpensive embossed plastic gratings. Typically such gratings are on aluminized substrates and used in the reflection mode of diffraction. One interesting feature of these gratings is their ability to diffract at grazing angles.

We show an experiment that is matched to the prediction of Figures 8 & 9. The setup for the experiment used a fiber optic line illuminator as a test target. It was inclined as a ramp. The camera was a single chip color camera with separate outputs for each primary. The lens and camera were placed at 75 degrees, near grazing exodus, relative to a grating of 600 nm pitch. This grating is a low cost embossed plastic grating with a glue backing attached to a piece of window glass. The setup is annotated in Figure 12. The camera output itself is shown in Figure 13.

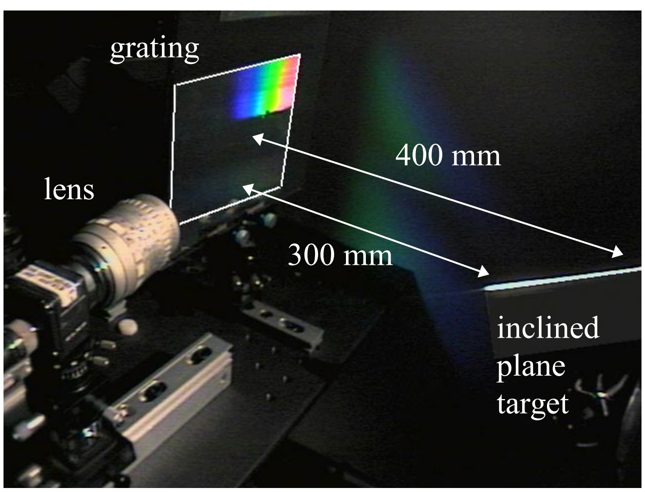

Figure 12 Bench setup for an experiment testing the mathematical model

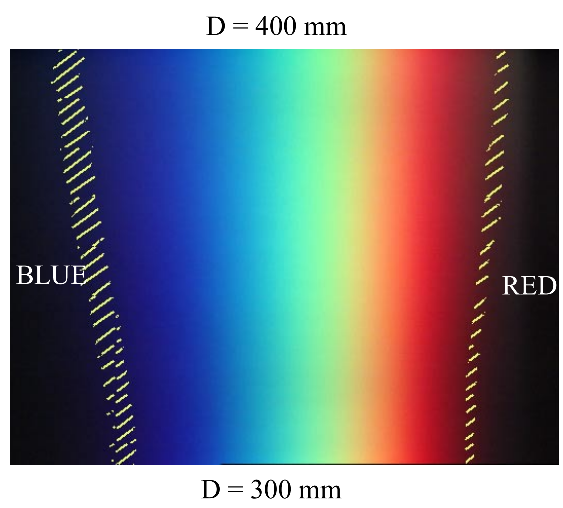

Figure 13 Spectra of inclined plane target taken with the experimental setup. Hatching is at the wave lengths (λ_1 = 420 nm and λ_2 = 650 nm) used in the calculation. Note that the spectral spread increases as the target distance increases.

Unlike triangulation systems, the chromatic diffraction range finding method produces an increase in sampled data as the target recedes. In the example of Figure 13, the most distant portion of the target is seen at the top of the frame. When all the available samples along a video line are used to statistically measure a target range, the availability of additional samples with greater distance overcomes the perspective foreshortening endemic to all triangulation and stereo range finding methods

A graph of the blue, green and red components of the video lines at the top, middle and bottom of the frame in Figure 13 are shown in Figure 14.

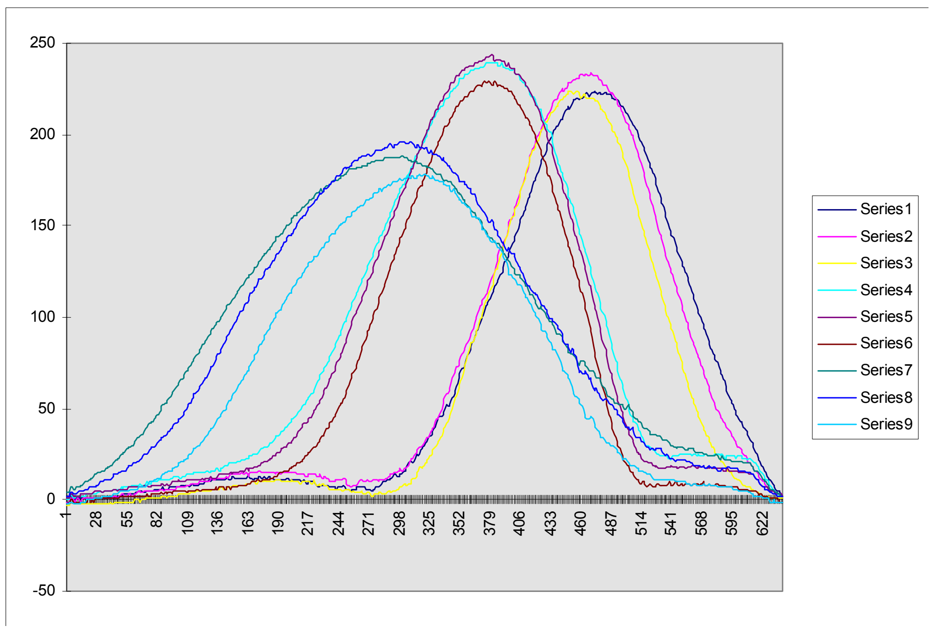

Figure 14 The Blue, Green and Red video lines of samples from the top, middle and bottom of Figure 13

CONCLUSION

The chromatic diffraction range finding method can be used to localize the spatial position of a target that radiates broadband illumination. The behavior conforms to geometric optics that follow the diffraction equation. A plurality of sampling points is available. The number of samples increases with target distance, reversing loss of resolution with distance that is endemic to triangulation and stereo. The plurality of samples also can overcome occlusion liability. The grating can be made from embossed plastic and is robust at a grazing exodus angles that allow for a compact configuration of the device.

References

[1] Thomas De Witt, US Patent 4,678,324, "Range Finding by Diffraction, July 7, 1987

[2] Tom Ditto and Douglas A. Lyon, "Moly - a prototype handheld three-dimensional digitizer with diffraction optics," *Optical Engineering*, January 2000, Vol 39 No. 1, pp. 68-78

[3] Tom Ditto, "Compact 3D Profilometer with Grazing Incidence Diffraction Optics," *Proceedings of the Third International Conference on 3-D Digital Imaging and Modeling*, IEEE Computer Society, PR00984, June 2001 pp. 73-80

[4] Tom DeWitt, (a.k.a. Tom Ditto), Pantograph, 1977 and 1979 (with Phil Edelstein), available at www.experimentaltvcenter.org/history/tools/tools_list.php3

[5] Tajima, Johji, et al., "3-D Data Acquisition by Rainbow Range Finder," *10th International Conference on Pattern Recognition*, pp. 309-313 (Jun. 1990)

[6] http://www.genextech.com/products_services/rainbow/overview.html

[7] Morovic J. and Morovic P. (2002) Input Imaging Media And Their Theoretical Colour Gamuts, *Color in Graphics Imaging and Vision* (CGIV), pp. 554-559